Cyclic Wiener Filtering: Theory and Method

William A. Gardner, *Fellow, IEEE*

Abstract—**Conventional time and space filtering of stationary random signals, which amounts to forming linear combinations of time translates and space translates, exploits the temporal and spatial coherence of the signals. By including frequency translates as well, the spectral coherence that is characteristic of cyclostationary signals can also be exploited. This paper develops some of the theoretical concepts underlying this generalized type of filtering called *FREquency-SHift (FRESH) filtering*, summarizes the theory of optimum FRESH filtering, which is a generalization of Wiener filtering called *cyclic Wiener filtering*, and illustrates the theory with specific examples of separating temporally and spectrally overlapping communications signals, including AM, BPSK, and QPSK. The structures and performances of optimum FRESH filters are presented, and adaptive adjustment of the weights in these structures is discussed. Also, specific results on the number of digital QAM signals that can be separated, as a function of excess bandwidth, are obtained.**

I. Introduction

In view of the tremendous diversity of theory, analytical technique, and method of implementation in the field of filtering, the objective of filtering seems almost trivial: viewed in the time-domain, the objective is to convolve a signal with an impulse-response function, which means to add up weighted versions of delayed replicas of the signal. Viewed in the frequency domain, the objective is to multiply the spectral components of the signal by a transfer function, which means to scale their strengths and shift their phases. Nevertheless, we know that this simple signal processing operation can perform the important task of mitigating the ill effects of both additive signal corruption, due to noise and interfering signals, and signal distortion, due to time-smearing phenomena such as dispersion and multipath propagation.

It is clear from the frequency domain viewpoint that signals can be separated from noise or interfering signals by filtering when the spectral content of the signal lies in a different band from that of the corruption. But another way to understand how a filter discriminates against corruption is to observe that if a signal is correlated with a time-shifted version of itself then, by adding a weighted version of the time-shifted signal to the original signal, the signal strength can be increased or decreased depending on the weight used. Thus, by choosing appropriate delays and weights, a signal can be enhanced while an interfering signal or noise is attenuated, provided that the correlations of the interference or noise differ from that of the signal.

This principle of exploiting temporal correlation or temporal coherence for signal selectivity has a spatial counterpart that is the basis for the spatial filtering capability of sensor arrays, which add up weighted space-shifted versions of signals. Thus, some of the theory, analytical techniques, and methods of implementation, such as those developed for adaptive digital filtering, carry over at least in part from time-filtering to array processing or, more generally, to joint time/space filtering by exploitation of temporal/spatial coherence [1].

A much lesser known generalization of time-filtering arises from the fact that for many man-made signals encountered in communications, radar, sonar, and telemetry systems, certain frequency-shifted versions of the signal can be highly correlated with the original signal. This spectral coherence can be exploited for signal selection by adding up properly weighted frequency-shifted versions of the signal.

For two reasons, the theory and practice of frequency-shift processing differs some from that of time-shift processing. First, the theory of time-invariant filtering based on exploiting temporal coherence is based primarily on the use of stationary time-series models for the signals and noises. This is so, for example, in the theory of Wiener filtering [2], [3]. Interestingly, no stationary time-series can exhibit spectral coherence and, consequently, frequency-shift processing is not useful for stationary time-series. Second, whereas temporal coherence is typically distributed continuously with the time-shift parameter, spectral coherence by its nature must be discretely distributed with the frequency-shift parameter. Therefore, arbitrary time shifts are useful in time-shift processing, but only select frequency shifts are useful in frequency-shift processing.

Actually, these two differences are intimately related. In recent theoretical developments [3]–[6], it has been established that a signal can exhibit spectral coherence if and only if it is *cyclostationary*, and the discrete frequency shifts for which the spectral correlation is nonzero coincide with the cycle frequencies of cyclostationarity. That is, the only type of nonstationarity that gives rise to spectral coherence is cyclostationarity [7]. This link between cyclostationarity and spectral coherence is briefly reviewed in Section II.

The purpose of this paper is to develop some of the theoretical concepts underlying the generalization of filtering that consists of not only magnitude–weighting and phase-shifting, but also frequency-shifting of spectral components. As an abbreviation, this FREquency-SHift filtering is referred to as *FRESH filtering*. However, because of the underlying statistical property of cyclostationarity that is exploited by FRESH filtering, we refer to the theory of optimum FRESH

Paper approved by the Editor for Signal Design, Modulation, and Detection of the IEEE Communications Society. This work was supported in part by the National Science Foundation under Grant MIP-88-12902, and in part by ESL, Inc., with partial matching support from the California State MICRO Program. This paper was presented in part at Asilomar Conference on Signals, Systems, and Computers, Pacific Grove, CA, 1989 and 1990.

The author is with the Department of Electrical Engineering, University of California, Davis, CA 95616.

IEEE Log Number 9203583.

filtering as *cyclic Wiener filtering* theory. This theory generalizes Wiener's theory of optimum time-invariant filtering of stationary time-series to optimum polyperiodic (multiply-periodic) time-variant filtering of cyclostationary time-series.

The first general theoretical development of optimum filtering for cyclostationary time-series was presented in the 1972 Ph.D. dissertation [8] (see [9]). The applications considered then were restricted to a single cyclostationary signal with a single period of cyclostationarity in additive stationary noise. For such applications, the most dramatic performance improvements of the cyclic Wiener filter over the conventional time-invariant Wiener filter are realizable with standard communication receiver structures such as demultiplexors/Wiener filters/multiplexors, and matched-filter-banks/periodic-sampler-banks/multi-variate-sampled-data Wiener filters. However, for the more general applications considered in this paper, which include multiple cyclostationary signals and/or interferences, each with one or more periods of cyclostationarity, in additive stationary or cyclostationary noise, the polyperiodic filtering structures required are novel.

The first general development of the frequency-domain theory of cyclic Wiener filtering was presented in the 1985 book [3]. Both these pioneering treatments [3], [8], as well as the early 1980's work in [10]–[11] on the joint receiver/transmitter optimization problem, were based on the probabilistic theory of stochastic processes where performance is measured in terms of ensemble averaged squared error. In 1987, a dual frequency-domain theory based on a nonprobabilistic theory of time-series, where performance is measured in terms of time-averaged squared error, was introduced [5]. This time-averaged theory has the advantage of being much more closely linked with adaptive implementations of FRESH filters and, as a result, is less likely to lead the user into conceptual pitfalls associated with unnecessary abstractions such as cycloergodicity [12]. In order to better serve potential users of cyclic Wiener filtering theory, the nonprobabilistic approach has been used exclusively by this author and his colleagues in continuing work since 1987. This is in keeping with Wiener's original treatise on optimum filtering.[1] This continuing work includes Brown's 1987 Ph.D. dissertation [13], which generalizes the theory from real time-series to complex time-series, and the two recent conference papers [6], [17], which further develop the theory for specific types of communications and telemetry signals. Specifically, in [16] the spectral correlation theory of pulse-amplitude modulated (PAM) signals is used to give a novel frequency-domain interpretation of the standard matched-filter/periodic-sampler/sampled-data-filter structure that forms the basis for many adaptive digital receivers. This new interpretation reveals the capacity of this structure to exploit spectral coherence in the PAM signal to mitigate severe partial-band corruption due to either fading or interference. The spectral correlation theory is also used in [16] to show that two cochannel amplitude-modulated (AM) signals can be perfectly separated by exploiting spectral coherence regardless of the degree of spectral overlap or of the values of their bandwidths and carrier frequencies and phases. In [17], the spectral correlation theory of binary phase-shift-keyed (BPSK) and quaternary phase-shift-keyed (QPSK) signals is used to demonstrate the degree to which two such spectrally overlapping signals can be separated by exploiting spectral coherence, as a function of receiver complexity (the number of frequency shifts and associated time-invariant filters). In addition, an empirical study of adaptive FRESH filtering for communications signals (which uses the probabilistic framework from [3]) is reported in Reed's 1987 Ph.D. dissertation [14] (see [15]).

In this paper, a more expansive study of the problem of separating cochannel digital quadrature AM (QAM) signals is presented with emphasis on the special cases of AM, BPSK, and QPSK (and, equivalently, all digital QAM with amplitude/phase constellations exhibiting quadrantal symmetry, since their spectral correlation characteristics are identical to those of QPSK [5]).

In Section II, the basic definitions of cyclostationarity and spectral correlation are briefly reviewed. In Section III, the equivalence of polyperiodic filtering and FRESH filtering is briefly explained, and the optimum FRESH filtering equations for filtering design and filter performance evaluation are presented. In Section IV, the class of QAM signals and the special cases of AM, BPSK, and QPSK are reviewed, and the spectral correlation functions for these signals are presented. In Section V, the specific optimum FRESH filtering structures for AM, BPSK, and QPSK are determined, and in Section VII their mean-squared-error performance is numerically evaluated as a function of the particular frequency-shift values used in the FRESH filter. In Section VI, a graphical explanation of how FRESH filtering can separate spectrally overlapping signals is provided. In Section VIII, the capabilities of FRESH filters for separating multiple digital QAM signals such as QPSK are delineated, and finally in Section IX, the relative merits of waveform extraction and digital data extraction are discussed.

II. Spectral Correlation

A complex-valued time-series $x(t)$ is said to exhibit *cyclostationarity* (in the wide sense) if its lag-product waveform $w_\tau(t) = x(t+\tau/2)x^*(t-\tau/2)$(where * denotes complex conjugation) exhibits finite-strength additive sine-wave components that give rise to spectral lines in the spectrum of $w_\tau(t)$ for some values of the lag parameter τ. The amplitude and phase of such a spectral line are given by the magnitude and argument of the complex-valued Fourier coefficient

$$R_x^\alpha(\tau) \triangleq \langle x(t+\tau/2)x^*(t-\tau/2)\exp(-i2\pi\alpha t)\rangle \quad (1)$$

where $\langle\cdot\rangle$ denotes average over all time t, and α is the frequency of the spectral line. For $\alpha = 0$, the function $R_x^0(\cdot) \equiv R_x(\cdot)$ is the conventional nonprobabilistic autocorrelation function. For $\alpha \neq 0$, it is called the *cyclic autocorrelation function* with *cycle frequency* α [5]. A time-series $x(t)$ is also said to exhibit cyclostationarity if the *conjugate cyclic autocorrelation function*

$$R_{xx^*}^\alpha(\tau) \triangleq \langle x(t+\tau/2)x(t-\tau/2)\exp(-i2\pi\alpha t)\rangle \quad (2)$$

[1] Many present-day authors mistakenly believe that Wiener's theory was based on stochastic processes.

is not identically zero for $\alpha \neq 0$. $R_x^\alpha(\tau)$ is typically nonzero for bauded signals, with α equal to the baud rate and its harmonics, whereas $R_{xx^*}^\alpha(\tau)$ is typically nonzero for carrier-modulated signals with α equal to twice the carrier frequency, possibly plus or minus the baud rate and its harmonics [5].

The complex envelope of the spectral component of $x(t)$ at frequency ν with approximate bandwidth $1/T$ is given by

$$X_T(t,\nu) \triangleq \frac{1}{T}\int_{t-T/2}^{t+T/2} x(u)\exp(-i2\pi\nu u)\,du. \quad (3)$$

The frequency density of correlation of spectral components at frequencies $\nu = f + \alpha/2$ and $\nu = f - \alpha/2$ is, therefore, given by

$$S_x^\alpha(f) \triangleq \lim_{T\to\infty} T\langle X_T(t, f+\alpha/2)X_T^*(t, f-\alpha/2)\rangle \quad (4)$$

where $\langle\cdot\rangle$ again denotes average over all time t. It can be shown that this *spectral correlation density function* and the cyclic autocorrelation function are a Fourier transform pair [5],

$$S_x^\alpha(f) = \int_{-\infty}^{\infty} R_x^\alpha(\tau)\exp(-i2\pi f\tau)\,d\tau. \quad (5)$$

Similarly, for a pair of time-series $x(t)$ and $y(t)$, we have

$$S_{xy}^\alpha(f) = \int_{-\infty}^{\infty} R_{xy}^\alpha(\tau)\exp(-i2\pi f\tau)\,d\tau \quad (6)$$

where

$$R_{xy}^\alpha(\tau) \triangleq \langle x(t+\tau/2)y^*(t-\tau/2)\exp(-i2\pi\alpha t)\rangle, \quad (7)$$

$$S_{xy}^\alpha(f) \triangleq \lim_{T\to\infty} T\langle X_T(t, f+\alpha/2)Y_T^*(t, f-\alpha/2)\rangle. \quad (8)$$

For $\alpha = 0$, the function $S_x^0(\cdot) \equiv S_x(\cdot)$ is the conventional spectral density of time-averaged power, and $S_{xy}^0(\cdot) \equiv S_{xy}(\cdot)$ is the cross-spectral density. Consequently, (5) is the Wiener relation for $\alpha = 0$, and for $\alpha \neq 0$ it is called the *cyclic Wiener relation* [5].

III. Optimum FRESH Filtering

It is well known that optimum filters for stationary signals are time-invariant. Similarly, optimum filters for signals that exhibit cyclostationarity with a single period (or multiple incommensurate periods) are singly (multiply) periodically time-variant. A polyperiodic time-variant linear filter has input-output relation

$$y(t) = \int_{-\infty}^{\infty} h(t,u)x(u)\,du \quad (9)$$

where for each value of the age variable $\tau = t-u$, the impulse-response function $h(t,u)$ is a polyperiodic (almost periodic, cf. [18]) function of the time variable u, and can be expanded in a Fourier series

$$h(t,u) = \sum_\eta h_\eta(t-u)\exp(i2\pi\eta u). \quad (10)$$

In this series, the Fourier coefficients for each value of τ are given by the average

$$h_\eta(\tau) = \langle h(t+\tau,t)\exp(-i2\pi\eta t)\rangle$$

over all time t, and the sum in (10) ranges over all integer multiples of each fundamental frequency $1/T_0$ corresponding to each period T_0 of the filter. Substituting (10) into (9) yields the general input-output relation for polyperiodic linear filters:

$$y(t) = \sum_\eta \int_{-\infty}^{\infty} h_\eta(t-u)[x(u)\exp(i2\pi\eta u)]\,du.$$
$$= \sum_\eta h_\eta(t) \otimes x_\eta(t) \quad (11)$$

where $\otimes$ denotes convolution and $x_\eta(t) \triangleq x(t)\exp(i2\pi\eta t)$ is a frequency-shifted version of $x(t)$. Considering for the moment finite-energy signals, which are Fourier transformable, the Fourier transforms of both sides of (11) can be equated to obtain

$$Y(f) = \sum_\eta H_\eta(f)X(f-\eta). \quad (12)$$

Thus, the input is subjected to a number of frequency-shifting (by amount η) operations, each followed by a linear time-invariant filtering operation [with impulse-response function $h_\eta(\cdot)$ and transfer function $H_\eta(\cdot)$], and the results are added together. Consequently, polyperiodic filtering is equivalent to FRESH filtering (discussed in Section I). From this, we see that the periodic time variations in an optimum filter for a signal that exhibits cyclostationarity provide the means (viz., frequency shifting) by which the spectral coherence of such signals can be exploited.

It is well known that linear time-invariant filtering of a real signal is equivalent to linear time-invariant filtering of its analytic signal which in turn is equivalent to linear time-invariant filtering of its complex envelope. But, this is not true for time-variant filtering. In general, linear time-variant filtering of a real signal is equivalent to distinct linear time-variant filtering of each of the complex envelope (or analytic signal) and its complex conjugate. This is proved in [13]. Consequently, if complex signals are to be used, then the problems of optimum and adaptive time-variant polyperiodic filtering must be approached as bivariate filtering problems, where a signal and its conjugate are jointly filtered and then added together. This is referred to as *linear-conjugate-linear (LCL) filtering* [19], [20].

The general form for the LCL–FRESH filtering of a complex signal $x(t)$ to produce an estimate $\hat{d}(t)$ of some desired signal $d(t)$ is then [cf. (11)]

$$\hat{d}(t) = \sum_{m=1}^{M} a_m(t) \otimes x_{\alpha_m}(t) + \sum_{n=1}^{N} b_n(t) \otimes x^*_{-\beta_n}(t) \quad (13)$$

where $x_{\alpha_m}(t) = x(t)\exp(i2\pi\alpha_m t)$ and $x^*_{-\beta_n}(t) = x^*(t)\exp(i2\pi\beta_n t)$, and where M and N can be infinite. The filter is completely specified by the numbers M and N, values $\{\alpha_m\}$ and $\{\beta_n\}$ of the periodicity frequencies (or frequency-shift parameters), and the impulse-response functions $\{a_m(t)\}$ and $\{b_n(t)\}$, or their Fourier transforms—the transform functions—$\{A_m(f)\}$ and $\{B_n(f)\}$.

For specified $M, N, \{\alpha_m\}$, and $\{\beta_n\}$, the optimum LCL—FRESH filtering problem is equivalent to the multivariate (dimension = $M+N$) Wiener filtering problem [5].

Using the vector concatenations

$$\boldsymbol{h}(t) = [a_1(t), \cdots, a_M(t), b_1(t), \cdots, b_N(t)]'$$
$$\boldsymbol{z}(t) = [x_{\alpha_1}(t), \cdots, x_{\alpha_M}(t), x^*_{-\beta_1}(t), \cdots, x^*_{-\beta_N}(t)]', \quad (14)$$

(13) can be reexpressed as $\hat{d}(t) = \boldsymbol{h}'(t) \otimes \boldsymbol{z}(t)$, and the vector of transfer functions that minimizes the time-averaged squared error between $\hat{d}(t)$ and $d(t)$ is given by the solution to the $M + N$ simultaneous linear equations

$$\boldsymbol{S}'_{zz}(f)\boldsymbol{H}(f) = \boldsymbol{S}_{dz}(f) \quad (15)$$

where $\boldsymbol{S}_{zz}(f)$ and $\boldsymbol{S}_{dz}(f)$ are the auto- and cross-spectral density matrices obtained by Fourier transforming the correlations

$$\boldsymbol{R}_{zz}(\tau) \triangleq \langle \boldsymbol{z}(t + \tau/2)\boldsymbol{z}^\dagger(t - \tau/2)\rangle$$
$$\boldsymbol{R}_{dz}(\tau) \triangleq \langle d(t + \tau/2)\boldsymbol{z}^*(t - \tau/2)\rangle,$$

in which $(\cdot)^\dagger$ denotes transpose conjugate. Substituting the definition of $\boldsymbol{z}(t)$ in terms of $x(t)$ into (15) yields the equivalent optimum LCL–FRESH filtering equations:

$$\sum_{m=1}^{M} S_x^{\alpha_k - \alpha_m}\left(f - \frac{\alpha_m + \alpha_k}{2}\right) A_m(f) + \sum_{n=1}^{N} S_{xx^*}^{\beta_n - \alpha_k}\left(f - \frac{\beta_n + \alpha_k}{2}\right)^* B_n(f) = S_{dx}^{\alpha_k}\left(f - \frac{\alpha_k}{2}\right), \quad k = 1, 2, \cdots, M, \quad (16a)$$

$$\sum_{m=1}^{M} S_{xx^*}^{\beta_k - \alpha_m}\left(f - \frac{\alpha_m + \beta_k}{2}\right) A_m(f) + \sum_{n=1}^{N} S_x^{\beta_k - \beta_n}\left(-f + \frac{\beta_n + \beta_k}{2}\right) B_n(f) = S_{dx^*}^{\beta_k}\left(f - \frac{\beta_k}{2}\right), \quad k = 1, 2, \cdots, N, \quad (16b)$$

which are fully specified in terms of the spectral correlation density functions for $x(t)$ and $d(t)$.

The spectrum of the error $e(t) \triangleq \hat{d}(t) - d(t)$ whose mean squared value is minimized by the multivariate Wiener filter is [5]

$$S_e(f) = S_d(f) - \boldsymbol{S}^\dagger_{dz}(f)\boldsymbol{H}(f), \quad (17)$$

which can be expressed more explicitly as

$$S_e(f) = S_d(f) - \sum_{m=1}^{M} S_{dx}^{\alpha_m}\left(f - \frac{\alpha_m}{2}\right)^* A_m(f) - \sum_{n=1}^{N} S_{dx^*}^{\beta_n}\left(f - \frac{\beta_n}{2}\right)^* B_n(f). \quad (18)$$

The problem of selecting the best finite sets of frequency-shift parameters $\{\alpha_m\}$ and $\{\beta_n\}$ is an important one in practice, but it is not easy to characterize mathematically. This problem is addressed in Section V. On the other hand, if no constraint is put on the number of frequency shifts to be used, then a (possibly infinite) set that is guaranteed to yield the minimum attainable time-averaged squared error is that which contains all α_m for which either

$$S_x^{\alpha_k - \alpha_m}\left(f - \frac{\alpha_m + \alpha_k}{2}\right) \neq 0$$

for each f and α_k which

$$S_{dx}^{\alpha_k}\left(f - \frac{\alpha_k}{2}\right) \neq 0$$

or

$$S_{xx^*}^{\beta_k - \alpha_m}\left(f - \frac{\alpha_m + \beta_k}{2}\right) \neq 0$$

for each f and $\beta_k$for which

$$S_{dx^*}^{\beta_k}\left(f - \frac{\beta_k}{2}\right) \neq 0;$$

and all β_n for which either

$$S_{xx^*}^{\beta_n - \alpha_k}\left(f - \frac{\beta_n + \alpha_k}{2}\right) \neq 0$$

for each f and α_k for which

$$S_{dx}^{\alpha_k}\left(f - \frac{\alpha_k}{2}\right) \neq 0$$

or

$$S_x^{\beta_k - \beta_n}\left(-f + \frac{\beta_n + \beta_k}{2}\right) \neq 0$$

for each f and β_k for which

$$S_{dx^*}^{\beta_k}\left(f - \frac{\beta_k}{2}\right) \neq 0.$$

This follows directly from (16a)–(16b).

For purely stationary signals,[2] we have [5]

$$S_x^\alpha(f) \equiv S_{xx^*}^\alpha(f) \equiv S_{dx}^\alpha(f) \equiv S_{dx^*}^\alpha(f) \equiv 0 \quad (19)$$

for all $\alpha \neq 0$, and for $\alpha = 0$ we also have (for complex envelopes $x(t)$) [21]

$$S_{xx^*}^0(f) \equiv S_{dx^*}^0 \equiv 0. \quad (20)$$

Consequently, $M = 1, N = 0$, and $\alpha_1 = 0$ in the optimum FRESH filter (13), which reduces to the single convolution

$$\hat{d}(t) = a_0(t) \otimes x_0(t).$$

In this case (16) reduces to

$$S_x^0(f)A_0(f) = S_{dx}^0(f),$$

which yields the transfer function $A_0(f)$ for the conventional Wiener filter. Generalizing this terminology for cyclostationary signals, the optimum FRESH filter specified by (16) with $M, N, \{\alpha_m\}$, and $\{\beta_n\}$ optimally chosen is called the *cyclic Wiener filter*. When N or M or $\{\alpha_m\}$ or $\{\beta_n\}$ is constrained in any way that is suboptimal, the resultant minimum-time-averaged-squared error filter specified by (16) is a *constrained* optimum FRESH filter and should not be called a cyclic

[2]These are the nonprobabilistic counterparts of cycloergodic stationary stochastic processes [5].

Wiener filter. This is consistent with the fact that only the unconstrained time-invariant (noncausal or causal) optimum filter is appropriately called a Wiener filter.[3]

It follows from the derivation of the optimum FRESH filtering equations (16), in terms of multivariate Wiener filtering, that adaptive implementations of FRESH filters can easily be obtained from conventional multivariate adaptive filters. Thus, a basic adaptively adjustable structure is simply a parallel bank of $N + M$ frequency-shifting product modulators each followed by an FIR filter, the outputs of which are summed. The $N + M$ filters can be jointly adapted using standard algorithms such as LMS, RLS, and the more recent constant-modulus algorithms.

IV. QAM Signals

A real QAM signal is made up of two sine-wave carriers in quadrature (Q), each amplitude modulated (AM) with a time series:

$$d(t) = c(t)\cos(\omega_o t) + s(t)\sin(\omega_o t). \tag{21}$$

If $c(t)$ and $s(t)$ are analog message signals, $d(t)$ is called simply QAM. If $s(t)$ is proportional to $c(t)$, then $d(t)$ is called AM. If in this latter case the amplitude, which is proportional to $c(t)$, is a digital PAM message signal

$$c(t) = \sum_{r=-\infty}^{\infty} c_r p(t - rT_o - t_o), \tag{22}$$

then $d(t)$ is called an amplitude-shift-keyed (ASK) signal with keying rate $1/T_o$. Also, if the pulse $p(t)$ is a full-duty-cycle rectangular pulse, and the digital variables c_r are binary-valued with values of ± 1, then this binary ASK signal is equivalent to a BPSK signal. If $s(t)$ is not proportional to $c(t)$, but is also a binary PAM signal with full-duty cycle rectangular pulses, then $d(t)$ is a QPSK signal. If the pulses in the QPSK signal are not restricted to be rectangular, then $d(t)$ is a 4-ary digital QAM signal. More generally, (21) is called an M-ary digital QAM signal when the total number of states of the pair (c_r, s_r) is equal to M. The M states correspond to different amplitude shifts

$$|a_r| = \sqrt{c_r^2 + s_r^2}$$

and different phase shifts

$$\angle a_r = -\tan^{-1}\left(\frac{s_r}{c_r}\right).$$

For all signals in this general QAM class, the spectral correlation function is given by [5]

$$S_d^\alpha(f) = \frac{1}{4}\sum_{n=-1,1}[S_c^\alpha(f + nf_o) + S_s^\alpha(f + nf_o)] + ni[S_{sc}^\alpha(f + nf_o) - S_{cs}^\alpha(f + nf_o)]$$
$$+ \frac{1}{4}\sum_{n=-1,1}[S_c^{\alpha+2nf_o}(f) - S_s^{\alpha+2nf_o}(f)] + ni[S_{sc}^{\alpha+2nf_o}(f) + S_{cs}^{\alpha+2nf_o}(f)] \tag{23}$$

where $f_o = \omega_o/2\pi$ and

$$S_c^\alpha(f) = \frac{1}{T_o^2}P(f + \alpha/2)P^*(f - \alpha/2) \times \sum_{r,s=-\infty}^{\infty} S_{\tilde{c}}^{\alpha - r/T_o}(f - s/T_o + r/2T_o)e^{-i2\pi\alpha t_o} \tag{24}$$

in which $P(f)$ is the Fourier transform of $p(t)$ and $\tilde{c}(t)$ is any times-series[4] for which $\tilde{c}(rT_o) = c_r$.

For

$$s(t) = \sum_{r=-\infty}^{\infty} s_r q(t - rT_o - t_o), \tag{25}$$

we have an expression for $S_s^\alpha(f)$ that is analogous to (24).

In the case where c_r is a purely stationary discrete-time-series, (24) reduces to

$$S_c^\alpha(f) = \frac{1}{T_o^2}P(f + \alpha/2)P^*(f - \alpha/2) \cdot \sum_{s=-\infty}^{\infty} S_{\tilde{c}}(f - s/T_o + \alpha/2)e^{-i2\pi\alpha t_o} \tag{26}$$

for $\alpha = k/T_o$ for all integers k, and $S_c^\alpha(f) \equiv 0$ for all other values of α. Also, if c_r is a white sequence with variance $\sigma_{\tilde{c}}^2$, then

$$S_c^\alpha(f) = \frac{\sigma_{\tilde{c}}^2}{T_o}P(f + \alpha/2)P^*(f - \alpha/2)e^{-i2\pi\alpha t_o}. \tag{27}$$

In addition, if c_r and s_r are statistically independent zero-mean time-series (cf. [5]), then $S_{cs}^\alpha(f) \equiv S_{sc}^\alpha(f) \equiv 0$, and (23) reduces to

$$S_d^\alpha(f) = \frac{1}{4}\sum_{n=-1,1}[S_c^\alpha(f + nf_o) + S_s^\alpha(f + nf_o) + S_c^{\alpha+2nf_o}(f) - S_s^{\alpha+2nf_o}(f)]. \tag{28}$$

For AM with purely stationary amplitude $c(t)$, (28) reduces further to (letting $s(t) \equiv 0$)

$$S_d^\alpha(f) = \begin{cases} \frac{1}{4}S_c(f), & \alpha = \pm 2f_o \\ \frac{1}{4}S_c(f + f_o) + \frac{1}{4}S_c(f - f_o), & \alpha = 0 \end{cases} \tag{29}$$

and $S_d^\alpha(f) \equiv 0$ for all other values of α. For BPSK with $T_o f_o$ irrational, (28) with (27) substituted in reduces to

$$S_d^\alpha(f) = \frac{\sigma_{\tilde{c}}^2}{4T_o}[P(f + f_o + \alpha/2)P^*(f + f_o - \alpha/2) + P(f - f_o + \alpha/2)P^*(f - f_o - \alpha/2)]e^{-i2\pi\alpha t_o} \tag{30}$$

for $\alpha = k/T_o$ and

$$S_d^\alpha(f) = \frac{\sigma_{\tilde{c}}^2}{4T_o}P(f + \alpha/2 \pm f_o)P^*(f - \alpha/2 \mp f_o) \cdot e^{-i2\pi[(\alpha \pm 2f_o)t_o \pm 2\varphi_o]} \tag{31}$$

[3] Constrained optimum filters such as FIR filters are commonly but incorrectly referred to as Wiener filters by present-day authors. Wiener's theory of optimum filtering was developed for the more challenging infinite-dimensional problem of unconstrained filtering rather than the simpler finite-dimensional problem of constrained filtering [2].

[4] (24) can be reexpressed in terms of the spectral correlation function for the discrete-time-series c_r [5].

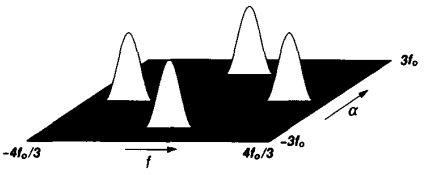

Fig. 1. Magnitude of spectral correlation function for an AM signal graphed as the height of a surface above the plane with coordinates f and α.

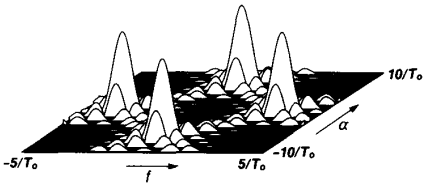

Fig. 2. Magnitude of spectral correlation function for a BPSK signal graphed as the height of a surface above the plane with coordinates f and α.

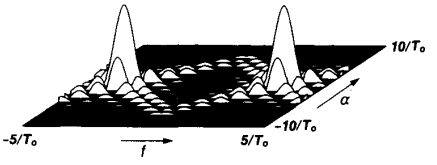

Fig. 3. Magnitude of spectral correlation function for a QPSK signal graphed as the height of a surface above the plane with coordinates f and α.

for $\alpha = \mp 2f_o + k/T_o$. The parameter φ_o is the carrier phase parameter which we have included in our BPSK model for the sake of generality,

$$d(t) = c(t)\cos(\omega_o t + \varphi_o). \tag{32}$$

For balanced QPSK (for which $S_c^\alpha(f) \equiv S_s^\alpha(f)$ and $S_{cs}^\alpha(f) \equiv 0$) with $T_o f_o$ irrational, we obtain (30) multiplied by 2 for $\alpha = k/T_o$, but $S_d^\alpha(f) \equiv 0$ for $\alpha = \mp 2f_o + k/T_o$.

The magnitude of these spectral correlation functions for AM, BPSK, and QPSK are graphed as the heights of surfaces above the plane with coordinates f and α in Figs. 1–3.

In the next section, only AM, BPSK, and balanced QPSK signals are considered, so only the results (29)–(31) are needed. However, both real signals and their complex representations are considered. For AM, the complex representation is simply

$$d(t) = a(t)e^{i(\omega_o t + \varphi_o)} \tag{33}$$

and for BPSK it is the same with

$$a(t) = \sum_{r=-\infty}^{\infty} a_r h(t - rT_o - t_o), \tag{34}$$

in which $a_r = c_r$ are real-valued, but $h(t)$ is, in general, complex-valued. For QPSK, (33)–(34) again apply, except that now $a_r = c_r - is_r$ are complex-valued. In both cases, (34) can be substituted into (33) to obtain

$$d(t) = \sum_{r=-\infty}^{\infty} b_r g(t - rT_o - t_o) \tag{35}$$

where

$$b_r = a_r e^{i[\omega_o(rT_0 + t_o) + \varphi_o]} \tag{36a}$$

and

$$g(t) = h(t)e^{i\omega_o t}. \tag{36b}$$

For this general complex digital QAM signal (35) where b_r is a white complex sequence with variance σ_b^2, the spectral correlation function is given by

$$S_d^\alpha(f) = \frac{\sigma_b^2}{T_o} G(f + \alpha/2)G^*(f - \alpha/2)e^{-i2\pi\alpha t_o} \tag{37}$$

for $\alpha = k/T_o$, and the conjugate spectral correlation function is given by

$$S_{dd^*}^\alpha(f) = \frac{\sigma_{\tilde{a}\tilde{a}^*}}{T_o} G(f + \alpha/2)G(\alpha/2 - f)e^{-i[2\pi(\alpha - 2f_o)t_o - 2\varphi_o]} \tag{38}$$

for $\alpha = 2f_o + k/T_o$ for BPSK, and for balanced QPSK we have

$$S_{dd^*}^\alpha(f) \equiv 0 \tag{39}$$

for all α.

Similarly, for the complex AM signal (33) where $c(t)$ is purely stationary and real-valued, the spectral correlation density function is given by

$$S_d^\alpha(f) = S_a(f - f_o), \quad \alpha = 0 \tag{40}$$

and $S_d^\alpha(f) \equiv 0$ for all $\alpha \neq 0$; the conjugate spectral correlation function is given by

$$S_{dd^*}^\alpha(f) = S_a(f)e^{i2\varphi_o}, \quad \alpha = 2f_o \tag{41}$$

and $S_{dd^*}^\alpha(f) \equiv 0$ for all $\alpha \neq 2f_o$.

In summary, the complex representation of AM has no spectral correlation; it has only conjugate spectral correlation (associated with the carrier frequency f_o). In contrast to this, the complex representation of balanced QPSK has no conjugate spectral correlation; it has only spectral correlation (associated with the baud rate $1/T_o$ and its harmonics). The complex representation of BPSK, on the other hand, has both spectral correlation and conjugate spectral correlation.

For all digital QAM signals whose amplitude/phase constellations exhibit quadrantal symmetry, the spectral correlation functions are identical to that of balanced QPSK.

For all three signals AM, BPSK, and QPSK, all spectral components with nonzero correlation are, in fact, completely correlated: their correlation coefficients

$$C_d^\alpha(f) \triangleq \frac{S_d^\alpha(f)}{[S_d(f + \alpha/2)S_d(f - \alpha/2)]^{1/2}} \tag{42}$$

have magnitude equal to unity, as explained in [5]. As a result of this spectral redundancy, certain spectral components in a signal can be used to completely cancel other spectral components in that signal. This is the primary mechanism that enables the separation of spectrally overlapping signals.

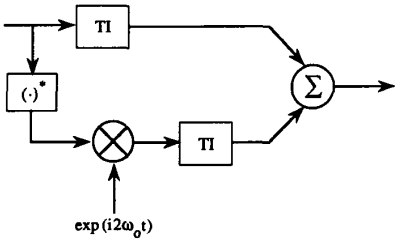

Fig. 4. LCL–FRESH-filter structure for an AM signal.

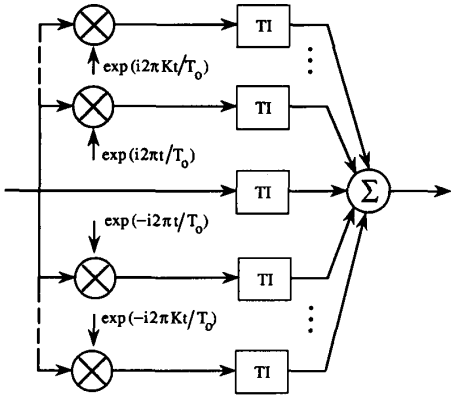

Fig. 5. FRESH-filter structure for a QPSK signal.

V. Optimum FRESH Filter Structures for QAM Signals

It follows from the results in Section IV for complex QAM signals and the optimum FRESH filtering equations (16) in Section III that in the LCL cyclic Wiener filter for AM in stationary noise, the linear (L) part does not include any frequency shifts—it includes only one time-invariant (TI) filter $(M = 1, \alpha_1 = 0)$—and the conjugate linear (CL) part includes only the one shift, $\beta_1 = 2f_o\,(N = 1, \beta_1 = 2f_o)$. This LCL–FRESH structure is shown in Fig. 4.

For QPSK in stationary noise, the results in Sections III and IV reveal that the LCL cyclic Wiener filter contains no CL part at all $(N = 0)$. The L part, however, includes frequency shifts $\alpha_m = m/T_o$ for all integers m for which

$$G(f + m/2T_o)G^*(f - m/2T_o) \not\equiv 0. \tag{43}$$

For 100 K% excess-bandwidth (EBW) pulses (i.e., 100 K% bandwidth in excess of the Nyquist bandwidth of $1/2T_o$), (43) requires $|m| \leq K$. Thus, in the L part of the filter there is a filtering path with no shift and there are also $\overline{K}$ parallel paths with positive shifts and another $\overline{K}$ with negative shifts (where $\overline{K}$ is the greatest integer that is less than or equal to K). Hence, for 100% EBW, the L part of the filter contains two frequency shifters, each followed by a TI filter, and there is a TI filter with no frequency shifter. For 200% EBW, there are four paths with frequency shifters and one path without, and so on. This L-FRESH structure is shown in Fig. 5.

For BPSK in stationary noise, the results in Sections III and IV reveal that the LCL cyclic Wiener filter contains the same paths in the L part as for QPSK, and it also contains the same number of paths in the CL part, but the frequency shift values are all increased by $2f_o$. In other words, each of the two TI filters in the structure for AM shown in Fig. 4 gets replaced for BPSK with a structure identical to that shown in Fig. 5, and both have the same $2\overline{K} + 1$ frequency shifts but different transfer functions.

The preceding results on frequency shifts can be arrived at quite easily by simply determining what shifts will yield overlapping spectral components from $x(t)$ and $d(t)$ that are correlated with each other. For the L part of the filter, we shift components in the spectrum of $x(t) = d(t) + n(t)$ where $n(t)$ is the noise, to overlap other components in the spectrum of $d(t)$. For the CL part, we shift components in the reversed spectrum of $x(t)$ to overlap components in the spectrum of $d(t)$. However, when there is more than one cyclostationary signal present, then we obtain not only the frequency shifts that are useful for each signal alone in stationary noise, but also sums and differences of some of these frequency shifts. The problem becomes sufficiently complicated, particularly when it is desired to find the optimum subset of a given size of all useful frequency shifts, that in the next section numerical evaluations of the mean-squared-error performance as a function of the particular frequency shifts used are resorted to. That is, the integral

$$\min\langle e^2(t)\rangle = \int_{-\infty}^{\infty} S_e(f)\,df \tag{44}$$

is numerically evaluated by first numerically solving the linear equations in (16) and substituting them into (18), the result of which is substituted into (44). However, before proceeding to the numerical study, a few cases that can be explained graphically are considered.

VI. Graphical Explanation of Signal Separation

To illustrate how two spectrally overlapping signals can be separated using FRESH filtering, we consider two cases. The first case involves two QPSK signals with unequal carrier frequencies and arbitrary baud rates, both of which have 100% EBW. Fig. 6, which shows the overlapping spectra of these two signals, illustrates graphically one way that exploitation of only cyclostationarity associated with the baud rate can be used to separate the two signals.

Starting from the top of this figure, each pair of graphs illustrates the result of one filtering and frequency-shifting stage. The subband shaded with a single set of parallel lines represents spectral components from one signal that are not corrupted by the other signal. These components are selected and complex-weighted by a filter and then frequency-shifted to cancel the components in another subband, which is identified by crosshatched shading. The result of this cancellation is shown in the second graph (which contains no shading) of each pair. The only frequency-shifts used are equal to plus and minus each of the two baud rates. After five such stages, a full sideband of each of the two QPSK signals has been completely separated. In each stage the spectral redundancy between complex spectral components separated by the baud

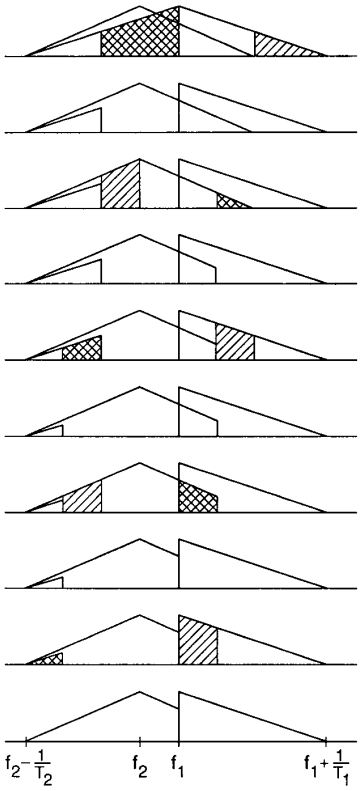

Fig. 6. Illustration of spectral densities for step-by-step separation of QPSK signals with unequal carriers and arbitrary baud rates, using baud-rate exploitation only.

rate is being exploited, and this same spectral redundancy can be used to reconstruct the entire QPSK from either one of its sidebands.

The five cascaded stages of filtering, frequency-shifting, and adding operations can be converted into one parallel connection of frequency shifters, each followed by a filter, simply by using standard system transformations to move all frequency shifters to the input.

Fig. 7 shows the overlapping spectra for the second case, which involves two AM (or BPSK) signals with unequal carrier frequencies and arbitrary bandwidths (or baud rates). The same scheme is used here to illustrate in a step-by-step manner how the two signals are separated. However, since the cyclostationarity associated with the carrier is being exploited in this case, and since the complex representations of the signals are being used, the operations involved in each step include a reflection of the subband shaded with a single set of parallel lines about the zero-frequency point before the complex weighting and shifting operations are applied. This extra operation corresponds to conjugating the time-domain signals. The only frequency-shifts used are equal to plus and minus each of the two carrier frequencies.

Although the graphical explanation of signal separation offered here requires that at least one of the signals be free of interference in some part of its band, this is not necessary in general. This is illustrated in Section VIII.

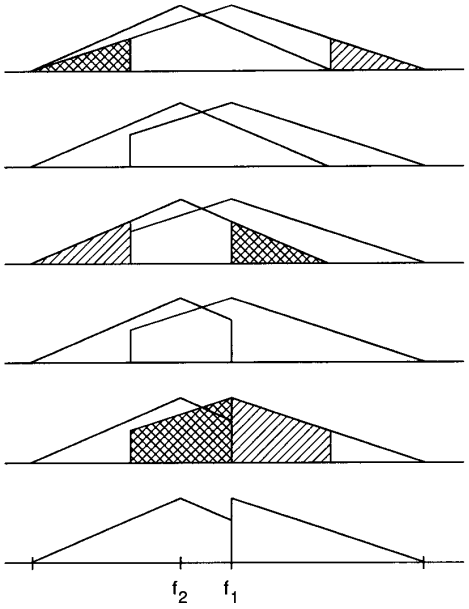

Fig. 7. Illustration of spectral densities for step-by-step separation of AM signals with unequal carriers, using carrier exploitation only.

VII. Performance of Optimum FRESH Filters for Interfering QAM Signals

In this section, sums of two or three real AM signals, or two complex BPSK signals, or two complex QPSK signals, in additive white Gaussian noise are considered. One of the two or three spectrally overlapping signals is considered to be the signal of interest (SOI), and the remaining one or two signals are considered to be signals not of interest (SNOI). All signals for each scenario considered have the same power spectral density, which is either triangle-shaped (for AM and BPSK/QPSK with 300% EBW), or raised-cosine-shaped (for BPSK/QPSK with 25% and 100% EBW),[5] the same EBW of either 25, 100, or 300%, and the same SNR of 20 dB. However, the absolute bandwidths, as determined by the baud rates, are the same in some cases and different in others. The same is true of the carrier frequencies.

In Figs. 8–10, the minimum mean-squared-error (MSE) in dB is shown versus the number of frequency shifts used in the complex LCL–FRESH filter for the case of the one SOI and one SNOI, both of which are either complex BPSK or complex QPSK. The values of the frequency-shifts used are specified in Table I for Fig. 8, Table II for Fig. 9, and Table III for Fig. 10. In these tables, the frequency shift having value 0 corresponds to the linear time-invariant (LTI) path for QPSK and it corresponds to both the LTI and LCLTI paths for BPSK. Similarly, for BPSK, each frequency-shift value listed is used in both the L and CL paths. There are no CL paths for QPSK. Thus, in terms of the number-of-shifts parameter L in Figs. 8–10, the number of actual filter paths for QPSK is $L+1$, but

[5] For BPSK and QPSK, these shapes are the squared magnitudes of the pulse transforms (keying-envelope transforms) since the digital data sequence is white. These particular shapes result in zero intersymbol interference at the output of a matched filter.

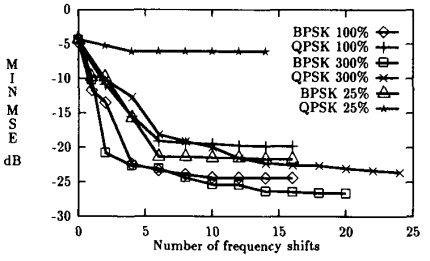

Fig. 8. Minimum MSE's for complex BPSK and QPSK signals with EBWs of 25%, 100%, and 300%, versus the number of frequency shifts used L. The SOI and SNOI have different baud rates and different carrier frequencies. SNOI overlaps the SOI 65%.

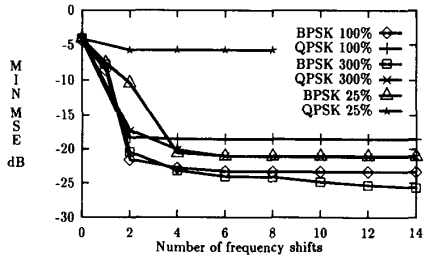

Fig. 9. Same as Fig. 6 except the baud rates are equal. SNOI overlaps the SOI 77%.

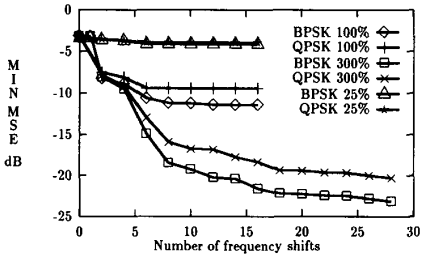

Fig. 10. Same as Fig. 6 except the carrier frequencies are equal. SNOI overlaps the SOI 75%.

for BPSK it is $2(L+1)$ for all $L > 1$, and it is $L+1$ for $L \leq 1$. However, since both the phases and frequencies of the two carriers are equal for the case depicted in Fig. 10, the CL path is of relatively little use for BPSK. The order of frequency shifts has been chosen empirically to maximize the rate of decrease of MSE with an increase in L. The carrier frequency and baud rate of the SOI are $f_* = 0$ and $f_1 = 1/(1+e)$ where $e = 1/4, 1, 3$ for excess bandwidths of 25, 100, and 300%, respectively. The two-sided bandwidth of the SOI is unity. In cases where the carrier frequency or baud rate of the SNOI are different from those of the SOI, their values are $f_0 = 0.2257$ and $f_2 = 0.753/(1+e)$, respectively, where 0.753 is the two-sided bandwidth of the SNOI. The triangular spectral densities for the three cases considered in Figs. 8–10 are shown in Fig. 11.

The best performance is attainable when the two carrier frequencies are different regardless of whether the baud rates are the same or different. The performance for these two cases

TABLE I
FREQUENCY-SHIFT VALUES IN THE ORDER THEY APPEAR IN FIG. 8. FREQUENCIES f_1 AND f_2 ARE THE BAUD RATES AND 0 AND f_0 ARE THE CARRIER FREQUENCIES OF THE SOI AND SNOI, RESPECTIVELY

QPSK 25%:	$0, \pm f_1, \pm f_2, \pm(f_1-f_2), \pm(f_1+f_2), \pm(2f_1-f_2), \pm(f_1-2f_2), \pm(2f_1-2f_2)$
BPSK 25%:	$0, \pm f_1, \pm f_2, \pm 2f_0, \pm(2f_0+f_2), \pm(2f_0-f_2), \pm(2f_0+f_1), \pm(2f_0-f_1), \pm(f_1-f_2)$
QPSK 100%:	$0, \pm f_1, \pm f_2, \pm(f_1-f_2), \pm(f_1+f_2), \pm(2f_1-f_2), \pm(f_1-2f_2), \pm 2(f_1-f_2), \pm 2(f_1+f_2)$
BPSK 100%:	$0, \pm f_1, \pm f_2, \pm(f_1-f_2), \pm 2f_0, \pm(2f_0-f_1), \pm(2f_0+f_1), \pm(2f_0-f_2), \pm(2f_0+f_2)$
QPSK 300%:	$0, \pm f_1, \pm f_2, \pm 2f_1, \pm(f_1-f_2), \pm(f_1+f_2), \pm(2f_1-f_2), \pm(f_1-2f_2), \pm 2(f_1-f_2), \pm 2(f_1+f_2), \pm(3f_1-2f_2), \pm(2f_1-3f_2), \pm 3f_1$
BPSK 300%:	$0, \pm f_1, \pm f_2, \pm 2f_0, \pm(2f_0+f_1), \pm(2f_0-f_1), \pm(2f_1-f_2), \pm 2f_1, \pm 2f_2, \pm 3f_1, \pm 3f_2$

TABLE II
FREQUENCY-SHIFT VALUES IN THE ORDER THEY APPEAR IN FIG. 9. FREQUENCY f_1 IS THE BAUD RATE FOR BOTH SOI AND SNOI, AND 0 AND f_0 ARE THE CARRIER FREQUENCIES OF THE SOI AND SNOI, RESPECTIVELY

QPSK 25%:	$0, \pm f_1, \pm 2f_1, \pm 3f_1, \pm 4f_1$
BPSK 25%:	$0, \pm f_1, \pm 2f_0, \pm(2f_0-f_1), \pm(2f_0+f_1), \pm 2f_1, \pm 3f_1$
QPSK 100%:	$0, \pm f_1, \pm 2f_1, \pm 3f_1, \pm 4f_1, \pm 2f_0, \pm(2f_0-f_1), \pm(2f_0+f_1)$
BPSK 100%:	$0, \pm f_1, \pm 2f_0, \pm(2f_0-f_1), \pm(2f_0+f_1), \pm 2f_1, \pm 3f_1, \pm 4f_1$
QPSK 300%:	$0, \pm f_1, \pm 2f_1, \pm 3f_1, \pm 4f_1, \pm 2f_0, \pm(2f_0-f_1), \pm(2f_0+f_1)$
BPSK 300%:	$0, \pm f_1, \pm 2f_1, \pm 3f_1, \pm 4f_1, \pm 2f_0, \pm(2f_0-f_1), \pm(2f_0+f_1)$

TABLE III
FREQUENCY-SHIFT VALUES IN THE ORDER THEY APPEAR IN FIG. 10. FREQUENCIES f_1 AND f_2 ARE THE BAUD RATES OF THE SOI AND SNOI, RESPECTIVELY, AND THE CARRIER FREQUENCIES OF BOTH THE SOI AND SNOI ARE ZERO

QPSK 25%:	$0, \pm f_1, \pm f_2, \pm(f_1-f_2), \pm(2f_1-f_2), \pm(f_1-2f_2), \pm 2(f_1-f_2), \pm(f_1+f_2), \pm 2(f_1+f_2)$
BPSK 25%:	$0, \pm f_1, \pm f_2, \pm(f_1-f_2), \pm(2f_1-f_2), \pm(f_1-2f_2), \pm 2(f_1-f_2), \pm(f_1+f_2), \pm 2(f_1+f_2)$
QPSK 100%:	$0, \pm f_1, \pm f_2, \pm(f_1-f_2), \pm(2f_1-f_2), \pm(f_1-2f_2), \pm 2(f_1-f_2), \pm(f_1+f_2), \pm 2(f_1+f_2)$
BPSK 100%:	$0, \pm f_1, \pm f_2, \pm(f_1-f_2), \pm(2f_1-f_2), \pm(f_1-2f_2), \pm 2(f_1-f_2), \pm(f_1+f_2), \pm 2(f_1+f_2)$
QPSK 300%:	$0, \pm f_1, \pm f_2, \pm(f_1-f_2), \pm(f_1+f_2), \pm 2f_1, \pm(2f_1-f_2), \pm(f_1-2f_2), \pm 2(f_1-f_2), \pm 2(f_1+f_2), \pm(3f_1-2f_2), \pm(2f_1-3f_2), \pm 3f_1, \pm 3f_2, \pm 2f_2$
BPSK 300%:	$0, \pm f_1, \pm f_2, \pm(f_1-f_2), \pm(f_1+f_2), \pm 2f_1, \pm(2f_1-f_2), \pm(f_1-2f_2), \pm 2(f_1-f_2), \pm 2(f_1+f_2), \pm(3f_1-2f_2), \pm(2f_1-3f_2), \pm 3f_1, \pm 3f_2, \pm 2f_2$

is shown in Figs. 8 and 9 where it can be seen that very little improvement relative to the LTI filter is available for QPSK with 25% EBW (since there is no spectral redundancy associated with the carriers and little associated with the baud rates because of the low EBW), but substantial improvement (14–16 dB) is available for QPSK with 100% EBW. For BPSK with 25% EBW, about 17–18 dB improvement is available, and this increases to about 20 dB for 100% EBW, and about

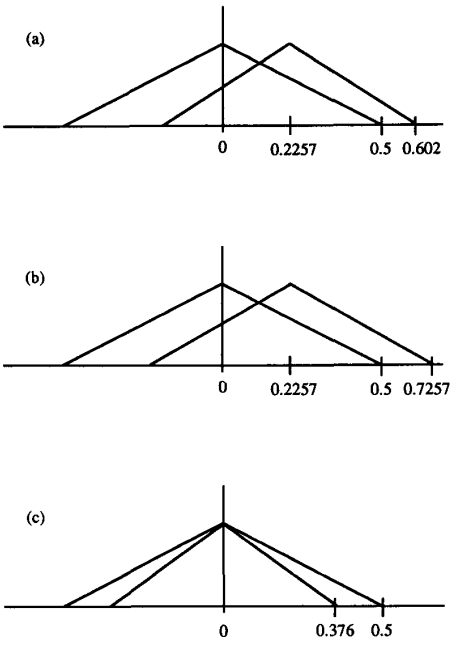

Fig. 11. The triangular spectral densities of the BPSK and QPSK signals used in Figs. 8–10. (a) Fig. 8. (b) Fig. 9. (c) Fig. 10.

22–23 dB for 300% EBW. Since the SNR is 20 dB, this reveals that the SNOI can be essentially eliminated for all EBW's for BPSK, but only for EBW $\geq$ 100% for QPSK.

The performance is not quite as good when the two carrier frequencies are the same and only the cyclostationarity associated with the baud rate is exploited unless the EBW exceeds 100%, but substantial improvement relative to the LTI filter is still attainable for EBWs on the order of 100%. The performance for this case is shown in Fig. 10, where it can be seen that there is little improvement relative to the LTI filter for either BPSK or QPSK when the EBW is low (25%). But, when the EBW is increased to 100%, an improvement of 6–7 dB is available, and this increases to 16–19 dB for EBW = 300%, in which case the SOI is very nearly eliminated. When the two phases of the carriers with equal frequencies are known, the cyclostationarity associated with the carriers can be exploited and amounts to using a slight variation on the conventional method for demodulating the in-phase and quadrature components of a QAM signal [13]. By this method the two signals can be perfectly separated. However, if the difference in the two phases is not sufficiently different from 0° or 180°, then the extracted signals will be severely attenuated, which will result in a substantial reduction in SNR. Also, when the carrier frequencies are different as in Figs. 8 and 9, but are close together, the large number of shifts required to separate the signals if the cyclostationarity of the baud rates is not exploited (e.g., if the signals are AM as in Fig. 12 and, therefore have no baud rate) can result in a substantial decrease in SNR.

In Fig. 12, the minimum MSE is shown versus the number of frequency shifts used in a real FRESH filter for one real AM SNOI and three cases of one or two real AM SNOI's.

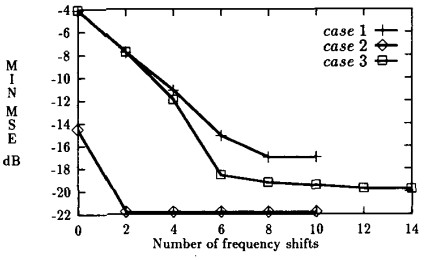

Fig. 12. Minimum MSE for real AM SOI and AM SNOIs versus the number of frequency shifts used. Case 1: $f_2 = 0.975, f_3 = 1.81$. Case 2: $f_2 = 1.55, f_3 = 1.9$. Case 3: $f_2 = 0.975$.

TABLE IV
FREQUENCY-SHIFT VALUES IN THE ORDER THEY APPEAR IN FIG. 12. FREQUENCY f_1 IS THE CARRIER FREQUENCY OF THE SOI AND f_2 AND f_3 ARE THE CARRIER FREQUENCIES OF THE TWO SNOI

Two SNOI, Cases 1, 2: $0, \pm 2f_1, \pm 2f_2, \pm 2(f_2-f_1), \pm 2(f_2-f_3), \pm 2(f_1-f_3)$
One SNOI, Case 3: $0, \pm 2f_1, \pm 2f_2, \pm 2(f_2-f_1), \pm 2(f_2-2f_1), \pm 2(2f_2-f_1), \pm 4(f_2-f_1), \pm 2(2f_2-3f_1)$

For cases 1 and 2, the first SNOI spectrally overlaps the real AM SOI and the second SNOI overlaps the first SNOI, but not the SOI. The amount of overlap of the SOI and first SNOI is 77 percent and the overlap of the first and second SNOI's is 16 percent for case 1. For case 2, the SOI and the first SNOI overlap 20% and the first and second SNOI's overlap 65%. For case 3, there is only one SNOI and it overlaps the SOI by 77%. The bandwidths of all three AM signals are unity, the carrier frequency of the SOI is $f_1 = 0.75$, and the carrier frequencies of the SNOI are denoted by f_2 and f_3. The particular values of frequency shifts used in Fig. 12 are shown in Table IV.

As can be seen from Fig. 12, excellent performance is attainable when there is only one SNOI, which overlaps the SOI by 77%. In this case (case 3) the SNOI is very nearly eliminated with the use of six frequency shifts. When two SNOI are present, one of which overlaps the SOI by 77%, about eight frequency shifts are needed to approach the best attainable performance (case 1). When there is only 20% overlap (case 2), the SNOI is essentially eliminated with only two frequency shifts. Similar results have been obtained for complex LCL–FRESH filtering of complex AM signals. Specifically, with $f_1 = 0, f_2 = 0.5, f_3 = 0.75$, and unity bandwidths (i.e., 50% overlap between first SNOI and SOI, and 75% overlap between the two SNOI), frequency shifts of $0, \pm 2f_2$ in both L and CL paths yield MSE = -21.5 dB. But, with $f_2 = 0.2257$ and $f_3 = 1.0$ (i.e., 77% overlap between first SNOI and SOI, and 23% overlap between the two SNOI), it takes nine frequency shifts (including combinations of both f_2 and f_3) in both L and CL paths to obtain MSE = -18.8 dB.

VIII. FRESH FILTERING CAPABILITIES FOR SEPARATION OF MULTIPLE QAM SIGNALS

The various scenarios of signal and interference considered in the previous section include no more than two overlapping signals at any one frequency. In this section, the more general

problem of an arbitrary number of spectrally overlapping signals is considered, but attention is restricted to only those signals that share a common baud rate $1/T_o$. Also, relatively large EBW's are considered since the number of signals that can be separated increases as the EBW is increased. Throughout the section, N signals are considered. Although the methods discussed apply for arbitrary carrier frequencies, the case of equal carrier frequencies is focused on since this is the worst case. To prevent the possibility of exploiting cyclostationarity associated with the carrier frequencies, digital QAM signals with quadrantal symmetry (like balanced QPSK) are considered.

Let us consider first the obvious situation where the N spectrally overlapping signals are disjoint in the time domain. That is, if the pulse envelopes are duration limited with widths of T_o/N (where T_o is the baud interval), and if the pulse epochs are equally staggered throughout the baud interval, then the signals do not overlap in time and can obviously be separated using periodically time-variant linear processing (time gating). The null-to-null bandwidth of each of these signals is $2N/T_o$, which corresponds to an approximate EBW of $(2N-1)$ 100% (the absolute bandwidth is infinite).

This simple result properly reflects the fact that to separate N spectrally overlapping signals, we need an EBW on the order of $100N\%$. However, it is shown in this section that there is no need to have the pulses perfectly staggered in time or nonoverlapping. In fact, it is shown that as long as their pulse-timings are distinct, and the EBW $\geq (N-1)$ 100%, they can be perfectly separated using FRESH filtering.

To gain insight into the problem of interest here, the signals are treated as if they were Fourier transformable (e.g., only a finite number of the random variables b_r in (35) are nonzero). From (35), we obtain the Fourier transform

$$D_n(f) = B_n(f)A_n(f)$$

where

$$B_n(f) \triangleq \sum_{r=-\infty}^{\infty} b_{nr}e^{-i2\pi rT_o f}$$
$$A_n(f) \triangleq G_n(f)e^{-i2\pi f t_n}$$
$$G_n(f) \triangleq \int_{-\infty}^{\infty} g_n(t)e^{-i2\pi ft}\,dt.$$

The factor $A_n(f)$ is nonrandom, but the factor $B_n(f)$ is random by virtue of the randomness of the digital data b_{nr}. The random factor is, however, periodic:

$$B_n(f + k/T_o) = B_n(f).$$

It follows that the random variables $D_n(f + k/T_o)$ for $k = 0, \pm 1, \pm 2, \cdots$ are perfectly correlated since they are simply scaled (by the nonrandom factors $A_n(f + k/T_o)$) versions of each other. Consequently, for each frequency f in the band $[-1/2T_o, 1/2T_o]$, the N frequency samples

$$X(f + k/T_o) = \sum_{n=1}^{N} A_n(f + k/T_o)B_n(f + k/T_o)$$
$$= \sum_{n=1}^{N} \left[\frac{A_n(f + k/T_o)}{A_n(f)}\right] D_n(f)$$

(for N integers k) of the transform of the received data

$$x(t) = \sum_{n=1}^{N} d_n(t)$$

produces N linear equations in the N unknowns $\{D_n(f): n = 1, 2, \cdots, N\}$. These equations can be solved if the $N \times N$ matrix with (kn)th element $A_n(f + k/T_o)$ is nonsingular. This can be guaranteed if the N pulse-timing parameters $\{t_n\}$ are different or if the N pulse shapes $\{g_n(t)\}$ are different. For example, if the n carrier frequencies ω_n in

$$g_n(t) = h_n(t)e^{i\omega_n t}$$

[from (36)] are different, then the matrix can be nonsingular even if the baseband pulse shapes $\{h_n(t)\}$ are all the same.

It should be pointed out that in the case being considered here, where the correlated spectral components are perfectly correlated (the correlation coefficient magnitudes are unity), we have been able to use a nonstatistical argument that completely circumvents the concept of correlation to obtain the desired result.[6] However, this nonstatistical argument is inadequate whenever the spectral correlation is imperfect (as it must be in practice). Furthermore, unlike the statistical theory presented here in Sections II–IV, the nonstatistical approach does not indicate how to optimize the FRESH filter to minimize MSE in arbitrary stationary and cyclostationary noise and interference backgrounds.

The solution described here in terms of solving N linear equations obtained from sampling in frequency can be implemented using a FRESH filter with N frequency shifts (one of which is zero) followed by an $N \times N$ matrix of TI filters. If the signals are BPSK instead of QPSK, then carrier exploitation also is possible by using an LCL structure. In this case, either more than N signals can be separated or the MSE for N signals in noise can be reduced.

IX. Waveform Extraction or Digital Data Extraction?

An issue that deserves some discussion is that of waveform extraction versus digital data extraction. That is, in a digital communication system, we ultimately are interested only in the quality of the extracted digital data, not the entire waveform that carries this data. However, in many cases the digital data can be obtained from the ideal transmitted waveform by time sampling at the baud rate, i.e., $d(rT_o + t_o) = a_r$ in (34). Even if the zero-intersymbol-interference criterion is not satisfied by the transmitted waveform, the training waveform used in an adaptive implementation can be constructed (e.g., from the

[6] A similar result is obtained in [23] using a nonstatistical argument. However, the result is for separation of the N digital data sequences only, not the entire signal waveforms (cf. Section IX herein).

data sequence a_r obtained at the output of a decision device) to satisfy this criterion. Furthermore, the cyclic Wiener filter specified by (16) minimizes the time-averaged squared error for all sequences of such time samples, regardless of sampling phase, since it is the optimum polyperidioc time-variant filter. Thus, when the number of frequency shifts used is enough to yield an MSE that closely approximates the absolute minimum, which is reached by the cyclic Wiener filter, the corresponding optimum FRESH filter for waveform extraction whose output is sampled at the times $t = rT_o + t_o$ will provide optimum extraction of the digital data. Moreover, it can be shown that the cyclic Wiener filter for the signal (34) provides the waveform estimate

$$\hat{d}(t) = \sum_{r=-\infty}^{\infty} \hat{b}_r g(t - rT_o - t_o)$$

where $\hat{b}_r$ is the minimum-MSE estimate of b_r, regardless of whether or not $d(rT_o + t_o) = b_r$ (cf. [22]). Thus, the cyclic Wiener filter can be followed by the ideal noise-free demodulator for this modulated signal. But it would probably be preferable to design $g(t)$ in a training signal $d(t)$ to guarantee not only $d(rT_o + t_o) = b_r$ but also small error $d(rT_o + t_o + \varepsilon) - b_r$ for the magnitude of time-sampling error ε that can be expected. The fact[7] that the cyclic Wiener filter minimizes MSE at all times t could then yield a small MSE even in the presence of unknown time sampling error.

On the other hand, by adaptively adjusting the filters to minimize the MSE at only $rT_o + t_o + \varepsilon$ where ε is an unknown timing offset, the FRESH filter will adapt to accommodate this timing offset provided that it varies sufficiently slowly. [The same is true for the optimum waveform extractor with timing offset in $d(t)$.] More importantly, when the number of frequency shifts used is less than the number needed to reach the performance of the cyclic Wiener filter, then lower MSE at the sampling times $t = rT_o + t_o + \varepsilon$ can potentially be obtained by ignoring the MSE at other times. Thus, by using decision direction to perform the adaptation, the MSE in estimating the digital data a_r is minimized (subject to the constraints imposed on the structure, such as the number of frequency shifts) independent of any zero-intersymbol-interference criterion.

In conclusion, when FRESH filters are actually implemented in practice, the best performance might be obtained by sampling the FRESH filter output at the baud rate and minimizing the MSE at these time samples only, using training data b_r or decision direction. However, without knowing more about the nature of the time-sampling error, it cannot be known for sure if this is so, or if the waveform estimator, which minimizes MSE for all time, might perform better.

It is worth mentioning at this point that when a bandlimited FRESH filter with frequency shifts equal to a baud rate and its harmonics only is followed by a baud-rate sampler, the overall structure is exactly equivalent to a fractionally spaced equalizer (with an unlimited number of equalizer taps) [16]. However, when incommensurate frequency shifts associated with multiple signals are used in the FRESH filter, no such equivalence is possible. In this sense, the FRESH filter, followed by a baud-rate sampler, is a generalization of the fractionally spaced equalizer.

It should also be pointed out that frequency-domain implementations of FRESH filters, based on the FFT, can be attractive alternatives [5]. The only difference between a frequency-domain implementation of a conventional TI filter and that of a polyperiodic (FRESH) filter is that the contents of more than one frequency bin from the input are linearly combined to obtain the contents of each frequency bin at the output. This idea has been pursued for digital data extraction (demodulation) as well as waveform extraction [24]–[26].

[7] This fact is not quite so obvious in the nonprobabilistic framework [5] adopted here as it is in the probabilistic framework [3].

X. Conclusion

In this paper, Wiener filtering theory is generalized from stationary signals to cyclostationary signals. The generalized optimum filters, called *cyclic Wiener filters,* are polyperiodic time-variant linear filters which incorporate frequency-shifting operations as well as the usual frequency-dependent amplitude-weighting and phase-shifting operations. It is shown that these frequency-shift filters can separate signals that overlap in frequency as well as in time. The minimum-MSE performance of these filters as a function of the number of frequency-shifts used is evaluated for several signal and interference scenarios. Specific results are obtained for the number of cochannel digital QAM signals that can be separated, as a function of their excess bandwidth. The results obtained show that the spectral redundancy inherent in excess bandwidth can be used effectively to improve system performance, and this suggests that excess bandwidth is a richer system-design parameter than previously recognized. In other words, high bandwidth-efficiency can be more costly in system performance when cochannel interference is present than we might have thought.

More recent work by the author has led to novel FRESH filtering structures that can be blindly adapted using only LS, RLS, or LMS algorithms, and with prior knowledge of only the modulation types and the values of carrier frequencies or baud rates, that is, without use of decision, direction, modulus restoral, or demodulation/remodulation methods, all of which exhibit threshold effects.

Acknowledgment

The author expresses his gratitude to Dr. S. V. Schell and Mr. S. Venkataraman for their assistance with the numerical evaluations of minimum mean squared error for FRESH filters that are presented in the figures.

References

[1] B. D. Van Veen and K. M. Buckley, "Beamforning: A versatile approach to spatial filtering," *IEEE ASSP Mag.,* vol. 5, pp. 4–24, Apr. 1988.

[2] N. Wiener, *Extrapolation, Interpolation, and Smoothing of Stationary Time Series, with Engineering Applications.* New York: Technology Press and J. Wiley, 1949. (Originally issued in February 1942, as a classified National Defense Research Council Report.)

[3] W. A. Gardner, *Introduction to Random Processes with Applications to Signals and Systems.* New York: Macmillan, 1985; also second ed., New York: McGraw-Hill, 1989.

[4] ——, "The spectral correlation theory of cyclostationary time-series," in *Signal Processing,* vol. 11, pp. 13–36, 1986. Errata: vol. 11, p. 405, 1986. (Also, in the RHS of (126b) and (126c), the factor 4 should be inserted.)
[5] ——, *Statistical Spectral Analysis: A Nonprobabilistic Theory.* Englewood Cliffs, NJ: Prentice-Hall, 1987.
[6] ——, "Exploitation of spectral redundancy in cyclostationary signals," *IEEE Signal Processing Mag.,* vol. 8, pp. 14–36, Apr. 1991.
[7] W. A. Gardner, "On the spectral coherence of nonstationary processes," *IEEE Trans. Signal Processing,* vol. 39, pp. 424–430, Feb. 1991.
[8] ——, "Representation and estimation of cyclostationary processes," Ph.D. dissertation, Dep. Elec. Comput. Eng., Univ. Massachusetts, Amherst, MA, 1972.
[9] W. A. Gardner and L. E. Franks, "Characterization of cyclostationary random signal processes," *IEEE Trans. Inform. Theory,* vol. IT-21, pp. 4–14, 1975.
[10] T. H. E. Ericson, "Modulation by means of linear periodic filtering," *IEEE Trans. Inform. Theory,* vol. IT-27, pp. 322–327, 1981.
[11] F. K. Graef, "Joint optimization of transmitter and receiver for cyclostationary random signal processes," in *Proc. NATO Advanced Study Inst. Nonlinear Stochast. Problems,* Algarve, Portugal, May 16–28, 1982, Dordrecht, Netherlands: Reidel, pp. 581–592.
[12] W. A. Gardner, "Common pitfalls in the application of stationary process theory to time-sampled and modulated signals," *IEEE Trans. Commun.,* vol. COM-35, pp. 529–534, 1987.
[13] W. A. Brown, "On the theory of cyclostationary signals," Ph.D. dissertation, Dep. Elec. Eng. Comput. Sci., Univ. California, Davis, 1987.
[14] J. H. Reed, "Time-dependent adaptive filters," Ph.D. dissertation, Dep. Elec. Eng. Comput. Sci., Univ. California, Davis, CA, Dec. 1987.
[15] J. H. Reed and T. C. Hsia, "The performance of time-dependent adaptive filters for interference rejection," *IEEE Trans. Acoust., Speech, Signal Processing,* vol. 38, pp. 1373–1385, Aug. 1990.
[16] W. A. Gardner and W. A. Brown, "Frequency-shift filtering theory for adaptive co-channel interference removal," in *Proc. Twenty-Third Annu. Asilomar Conf. Signals, Syst., Comput.,* Pacific Grove, CA, Oct. 30–Nov. 1, 1989, pp. 562–567.
[17] W. A. Gardner and S. Venkataraman, "Performance of optimum and adaptive frequency-shift filters for co-channel interference and fading," in *Proc. Twenty-Fourth Annu. Asilomar Conf. Signals, Syst., Comput.,* Pacific Grove, CA, Nov. 5–6, 1990, pp. 242–247.
[18] C. Corduneaunu, *Almost Periodic Functions.* New York: Wiley, 1961.
[19] W. M. Brown, "Conjugate linear filtering," *IEEE Trans. Inform. Theory,* vol. IT-15, pp. 462–465, 1969.
[20] W. M. Brown, *Analysis of Linear Time-Invariant Systems.* New York: McGraw-Hill, 1963.
[21] N. R. Goodman, "Statistical analysis based on a certain multivariate complex Gaussian distribution (an introduction)," *Ann. Math. Stat.,* vol. 34, pp. 152–177, 1963.
[22] W. A. Gardner, "The structure of linear least-mean-square estimators for synchronous M-ary signals," *IEEE Trans. Inform. Theory,* vol. IT-19, pp. 240–243, 1973.
[23] M. Abdulrahman and D. D. Falconer, "Cyclostationary crosstalk suppression by decision feedback equalization on digital subscriber loops," *IEEE J. Select. Areas Commun.* vol. 10, pp. 640–649, 1992.
[24] E. R. Ferrara, "Frequency-domain implementations of periodically time-varying filters," *IEEE Trans. Acoust., Speech, Signal Processing,* vol. ASSP-33, pp. 883–892, 1985.
[25] J. H. Reed, C. D. Greene, and T. C. Hsia, "Demodulation of a direct sequence spread-spectrum signal using an optimal time-dependent receiver," in *1989 IEEE Military Commun. Conf.*, Boston, MA, Oct. 1989.
[26] B. G. Agee and S. V. Venkataraman, "Adaptive demodulation of PCM signals in the frequency domain," in *Proc. Twenty-Third Annu. Asilomar Conf. Signals, Syst., Comput.,* Pacific Grove, CA, Oct. 30–Nov. 1, 1989.

William A. Gardner (S'64–M'67–SM'84–F'91) was born in Palo Alto, CA, on November 4, 1942. He received the M.S. degree from Stanford University, in 1967, and the Ph.D. degree from the University of Massachusetts, Amherst, in 1972, both in electrical engineering.

He was a Member of the Technical Staff at Bell Laboratories in MA, from 1967 to 1969. He has been a faculty member at the University of California, Davis, since 1972, where he is Professor of Electrical Engineering and Computer Science. Since 1982, he has also been President of the engineering consulting firm Statistical Signal Processing, Inc., Yountville, CA. His research interests are in the general area of statistical signal processing, with primary emphasis on the theories of time-series analysis, stochastic processes, and signal detection and estimation and applications to communications and signals intelligence.

Dr. Gardner is the author of *Introduction to Random Processes with Applications to Signals and Systems,* Macmillan, New York, 1985, second edition, McGraw-Hill, New York, 1990, *The Random Processes Tutor: A Comprehensive Solutions Manual for Independent Study,* McGraw-Hill, New York, 1990, and *Statistical Spectral Analysis: A Nonprobabilistic Theory,* Prentice-Hall, Englewood Cliffs, NJ, 1987. He holds several patents and is the author of numerous research-journal papers. He received the Best Paper of the Year Award from the European Association for Signal Processing in 1986 for the paper entitled "The spectral correlation theory of cyclostationary signals," the 1987 Distinguished Engineering Alumnus Award from the University of Massachusetts, and the Stephen O. Rice Prize Paper Award in the Field of Communication Theory from the IEEE Communications Society in 1988 for the paper entitled "Signal interception: A unifying theoretical framework for feature detection." He organized and chaired the NSF/ONR/ARO/AFOSR-sponsored workshop on Cyclostationary Signals, 1992. He is a member of the American Association for the Advancement of Science, the European Association for Signal Processing, and a member of the honor societies Sigma Xi, Tau Beta Pi, Eta Kappa Nu, and Alpha Gamma Sigma.